DOI: 10.1007/s12541-012-0207-z

Dynamic Behavior of Overhung Rotors Subjected to Axial Forces

Kyung Bin Yim[1,#] and John Yim[2]

1 School of Mechanical Engineering, Dongyang Mirae University, 62-160, Gochuk-dong, Guro-gu, Seoul, South Korea, 152-714
2 NASA Glenn Research Center, 21000 Brookpark Road, Cleveland, OH 44135, USA
Corresponding Author / E-mail: kbyim@dongyang.ac.kr, TEL: +82-2-2610-1847, FAX: +82-2-2610-1852

KEYWORDS: Axial force, Dynamic behavior, Overhung rotor, Transfer matrix method

The dynamic behavior of a flexible shaft with a disk subjected to axial forces has been studied by employing the transfer matrix approach. The conventional transfer matrix was modified to include the applied axial force, and then integrated into a computer program to investigate the effect of the load force on the stability and the natural frequencies of overhung rotor systems. Two overhung rotor systems are considered. One is the cantilevered rotor and the other is the overhung rotor with an intermediate support. The gyroscopic effect of the rotor strongly influences the dynamic behavior of the shaft-disk system under axial forces not only by increasing the critical force for the stability but also by changing the instability type from divergence to flutter.

Manuscript received: September 23, 2011 / Accepted: March 15, 2012

NOMENCLATURE

E = Young's modulus
I = area moment of inertia of the shaft
Ω = shaft speed
P = applied axial force
ℓ = shaft length
m = distributed mass of the shaft per unit length
m_d = disk mass
I_p = polar moment of inertia of the shaft
I_p = polar moment of inertia of the disk
I_t = transverse moment of inertia of the shaft
I_t = transverse moment of inertia of the disk
V = shearing force
M = bending moment
ψ = angle tangent to the deflection curve

1. Introduction

Numerous analyses have been published on the subject of a beam under axial loads by various investigators.[1-4] Saito and Otomi[1] studied the vibration and stability of an elastically supported beam carrying an attached mass and subjected to axial and tangential compressive loads. They presented the influence of the support stiffness, the direction of loading, and the slenderness ratio on the natural frequency and critical load of a beam. Ari-Gul and Elishakoff[2] conducted an analysis on the shear-flexural buckling of columns with overhang under an axial force by solving the differential equations of static equilibrium at the onset of buckling for a Timoshenko-type beam. Wang et al.[3] presents the stability criteria and buckling loads of columns under intermediate and end concentrated axial loads by employing the Timoshenko column theory. They showed the effect of transverse shear deformation on the buckling capacity of the column under compressive loads. Arboleda-Monsalve et al.[4] performed the stability and free vibration analyses of a weakened Timoshenko beam-column with generalized end conditions under constant axial load. They presented the coupling effects of some factors such as shear and bending deformations along the member's span, the translational and rotational masses of the member uniformly distributed along its span, and constant axial load.

Many researchers studied also the effect of axial loads on a rotating shaft since an axial load can be easily generated in a real machine by the pressure difference across the rotor disk or in other applications.[5] Ku and Chen[6] used the finite element method to study the stability behavior and whirl speed of a rotating shaft subjected to an axial compressive load. They showed the variations of the whirl speed of a shaft as the axial compressive load increases and found that the critical instability load is independent of the spin speed of the shaft. Czolczynski and Marynowski[7] investigated the

stability of a rotating disk with a flexible shaft of negligible mass subjected to a longitudinal force acting on a disk and concluded that the critical axial force is practically independent of the support stiffness. Sheu and Chen[8] employed a lumped mass model to determine the regions of parametric instability of a cantilever shaft-disk system subjected to periodic longitudinal forces. They found that the periodic axial loading makes the rotor system more unstable than the periodic follower force does under the same static load factor.

This paper addresses the modeling and stability analyses of an overhung rotor subjected to an axial force by employing the transfer matrix method. The equation of motion of an overhung rotor under an axial end force is first derived. And then, a transfer matrix approach is presented for the dynamic analysis of a general rotor-bearing system under axial forces. Two different types of overhung rotor systems are considered to cover the typical overhung turbomachine.

2. Theoretical Development

2.1 Equations of Motion of a Cantilevered Overhung Disk under Axial Force

Fig. 1 depicts the cantilevered overhung rotor with speed Ω under applied axial force P. The kinetic energy of the entire shaft rotating speed of Ω is

$$K_s = \frac{1}{2}\int_0^{\ell}\left[m\left(\frac{\partial x}{\partial t}\right)^2 + m\left(\frac{\partial y}{\partial t}\right)^2 + \underline{I}_t\left\{\frac{\partial}{\partial t}\left(\frac{\partial x}{\partial z}\right)\right\}^2 + \underline{I}_t\left\{\frac{\partial}{\partial t}\left(\frac{\partial y}{\partial z}\right)\right\}^2 + \underline{I}_p\left\{\Omega^2 + 2\Omega\left\{\frac{\partial}{\partial t}\left(\frac{\partial x}{\partial z}\right)\right\}\left(\frac{\partial y}{\partial z}\right)\right\}\right] dz \tag{1}$$

The kinetic energy of the rotating disk is

$$K_d = \frac{1}{2}\left[m_d\left(\frac{\partial x}{\partial t}\right)^2 + m_d\left(\frac{\partial y}{\partial t}\right)^2 + I_t\left\{\frac{\partial}{\partial t}\left(\frac{\partial x}{\partial z}\right)\right\}^2 + I_t\left\{\frac{\partial}{\partial t}\left(\frac{\partial y}{\partial z}\right)\right\}^2 + I_p\left\{\Omega^2 + 2\Omega\left\{\frac{\partial}{\partial t}\left(\frac{\partial x}{\partial z}\right)\right\}\left(\frac{\partial y}{\partial z}\right)\right\}\right]_{\ell} \tag{2}$$

where the subscript ℓ represents the right end of the shaft.

The work due to the bending moment and a compressive axial load P becomes

$$W = -\frac{1}{2}\int_0^{\ell}\left[EI\left\{\left(\frac{\partial^2 x}{\partial z^2}\right)^2 + \left(\frac{\partial^2 y}{\partial z^2}\right)^2\right\} - P\left\{\left(\frac{\partial x}{\partial z}\right)^2 + \left(\frac{\partial y}{\partial z}\right)^2\right\}\right] dz \tag{3}$$

Substituting Eqs. (1)-(3) into the extended Hamilton's principle

$$\int_{t_1}^{t_2}(\delta K_s + \delta K_d + \delta W)dt = 0 \tag{4}$$

and introducing a complex deflection, $w = x + iy$, yield the following equation of motion

$$EI\frac{\partial^4 w}{\partial z^4} + P\frac{\partial^2 w}{\partial z^2} - \underline{I}_t\frac{\partial^4 w}{\partial z^2\partial t^2} + i\underline{I}_p\Omega\frac{\partial^3 w}{\partial z^2\partial t} + m\frac{\partial^2 w}{\partial t^2} = 0 \tag{5}$$

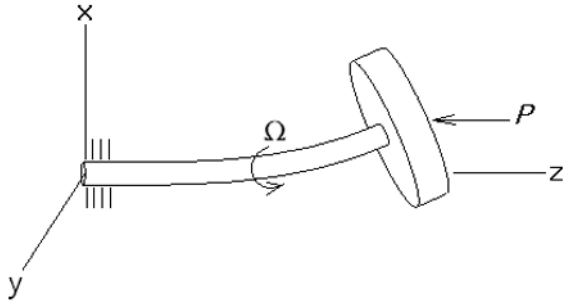

Fig. 1 Coordinates and axial compressive external force for the cantilevered overhung disk

with the associated boundary conditions at $z = 0$:

$$w = 0, \quad \frac{\partial w}{\partial z} = 0 \tag{6}$$

and at $z = \ell$:

$$EI\frac{\partial^3 w}{\partial z^3} + P\frac{\partial w}{\partial z} - m_d\frac{\partial^2 w}{\partial t^2} = 0 \tag{7a}$$

$$EI\frac{\partial^2 w}{\partial z^2} + I_t\frac{\partial^3 w}{\partial t^2\partial z} - iI_p\Omega\frac{\partial^2 w}{\partial t\partial z} = 0 \tag{7b}$$

Substituting the following nondimensional parameters

$$\eta = \frac{z}{\ell}, \quad v = \frac{w}{\ell}, \quad \tau = \Omega t, \quad \tilde{P} = \frac{P\ell^2}{EI}, \quad \tilde{\Omega}^2 = \frac{m}{EI}\ell^4\Omega^2,$$
$$m_R = \frac{m_d}{m\ell}, \quad \underline{I}_R = \frac{\underline{I}_p}{\underline{I}_t}, \quad I_R = \frac{I_p}{I_t}, \quad \underline{Q} = \frac{\underline{I}_t}{m\ell^2}, \quad Q = \frac{I_t}{m_d\ell^2}$$

into Eqs. (5)-(7) yields the dimensionless equations as

$$\frac{\partial^4 v}{\partial\eta^4} + \tilde{P}\frac{\partial^2 v}{\partial\eta^2} - \underline{Q}\tilde{\Omega}^2\frac{\partial^4 v}{\partial\eta^2\partial\tau^2} + i\underline{I}_R\underline{Q}\tilde{\Omega}^2\frac{\partial^3 v}{\partial\eta^2\partial\tau} + \tilde{\Omega}^2\frac{\partial^2 v}{\partial\tau^2} = 0 \tag{8}$$

where at $\eta = 0$

$$v = 0, \quad \frac{\partial v}{\partial\eta} = 0 \tag{9}$$

and at $\eta = 1$

$$\frac{\partial^3 v}{\partial\eta^3} + \tilde{P}\frac{\partial v}{\partial\eta} - m_R\tilde{\Omega}^2\frac{\partial^2 v}{\partial\tau^2} = 0 \tag{10a}$$

$$\frac{\partial^2 v}{\partial\eta^2} + m_R\underline{Q}\tilde{\Omega}^2\frac{\partial^3 v}{\partial\tau^2\partial\eta} - im_R\underline{Q}I_R\tilde{\Omega}^2\frac{\partial^2 v}{\partial\tau\partial\eta} = 0 \tag{10b}$$

Introducing a trial solution in series form

$$v(\eta,\tau) = \sum_{j=1}^{4} C_j\exp(r_j\eta + s\tau) \tag{11}$$

where s is a complex number to be determined, $s = \lambda \pm i\omega$. into Eqs. (8)-(10b) gives

$$r_j^4 + \tilde{P}r_j^2 - \underline{Q}\tilde{\Omega}^2 s^2 r_j^2 + i\underline{I}_R\underline{Q}\tilde{\Omega}^2 s r_j^2 + \tilde{\Omega}^2 s^2 = 0 \tag{12}$$

and four homogeneous equations in C_j. The necessary and sufficient condition for a nontrivial solution of four equations in C_j is that the determinant of the coefficients of C_j must be zero. Thus,

$$\Delta = \begin{vmatrix} 1 & 1 & 1 & 1 \\ r_1 & r_2 & r_3 & r_4 \\ f_1 e^{r_1} & f_2 e^{r_2} & f_3 e^{r_3} & f_4 e^{r_4} \\ g_1 e^{r_1} & g_2 e^{r_2} & g_3 e^{r_3} & g_4 e^{r_4} \end{vmatrix} = 0 \tag{13}$$

where

$$f_j = r_j^3 + \tilde{P} r_j - m_R \tilde{\Omega}^2 s^2$$
$$g_j = r_j^2 + m_R Q \tilde{\Omega}^2 s^2 r_j - i m_R Q I_R \tilde{\Omega}^2 s r_j$$

Equation (13) is the characteristic equation for the system shown in Fig. 1, subjected to an axial force. Eqs. (12) and (13) are used to check the numerical results obtained using the transfer matrix in 2.2.

2.2 Transfer Matrix Formulation

The conventional transfer matrix is modified to account for an axial force. Fig. 2 presents the sign convention for the *n*th station and the *n*th shaft section on the xz-plane.

The inertia transfer function at the *n*th station can be expressed in matrix form as

$$\begin{Bmatrix} x \\ y \\ \psi_x \\ \psi_y \\ V_x \\ V_y \\ M_x \\ M_y \end{Bmatrix}_n^R = \begin{bmatrix} 1 & 0 & 0 & 0 & 0 & 0 & 0 & 0 \\ 0 & 1 & 0 & 0 & 0 & 0 & 0 & 0 \\ 0 & 0 & 1 & 0 & 0 & 0 & 0 & 0 \\ 0 & 0 & 0 & 1 & 0 & 0 & 0 & 0 \\ -s^2 m & 0 & 0 & 0 & 1 & 0 & 0 & 0 \\ 0 & -s^2 m & 0 & 0 & 0 & 1 & 0 & 0 \\ 0 & 0 & s^2 I_t & s\Omega I_p & 0 & 0 & 1 & 0 \\ 0 & 0 & -s\Omega I_p & s^2 I_t & 0 & 0 & 0 & 1 \end{bmatrix} \begin{Bmatrix} x \\ y \\ \psi_x \\ \psi_y \\ V_x \\ V_y \\ M_x \\ M_y \end{Bmatrix}_n^L \tag{14}$$

In more compact form,

$$\{X\}_n^R = [T_m]_n \{X\}_n^L \tag{15}$$

where R and L denote right and left side of station *n*, respectively.

The following relationships can be obtained for the shaft section;

$$\begin{aligned} V_{x,n+1}^L &= V_{x,n}^R \\ M_{x,n+1}^L &= M_{x,n}^R + V_{x,n}^R \ell_n - P_n (x_{n+1} - x_n) \\ x_{n+1} &= x_n + \ell_n \psi_{x,n} - a_{xx} (V_{x,n}^R - P_n \psi_{x,n}) + a_{x\psi} M_{x,n+1}^L \\ \psi_{x,n+1} &= \psi_{x,n} - a_{\psi x} (V_{x,n}^R - P_n \psi_{x,n}) + a_{\psi\psi} M_{x,n+1}^L \end{aligned} \tag{16}$$

The same relationship can be obtained for y-z plane by replacing x with y in the above equations. Where the flexibility influence coefficients a_{ij} for a cantilevered beam under the axial force are found by using the method in reference[9] as

$$\begin{aligned} a_{xx} &= \frac{\ell}{P}\left(\frac{1}{k}\tan k - 1\right) \quad \text{where} \quad k = \left(\frac{P\ell^2}{EI}\right)^{1/2} \\ a_{x\psi} &= -a_{\psi x} = \frac{1}{P}\left(1 - \frac{1}{\cos k}\right) \\ a_{\psi\psi} &= \frac{k}{P\ell}\tan k \end{aligned} \tag{17}$$

The transfer function for the shaft section can be expressed in the following matrix form by combining Eqs. (16) and (17)

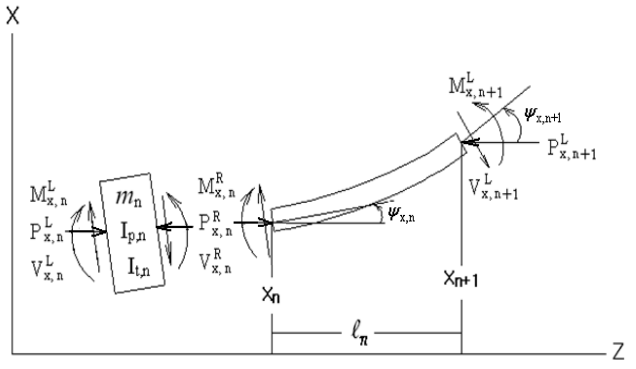

Fig. 2 Sign convention for the nth section on the xz-plane

$$\begin{Bmatrix} x \\ y \\ \psi_x \\ \psi_y \\ V_x \\ V_y \\ M_x \\ M_y \end{Bmatrix}_{n+1}^L = \begin{bmatrix} 1 & 0 & C_{13} & 0 & C_{15} & 0 & C_{17} & 0 \\ 0 & 1 & 0 & C_{24} & 0 & C_{26} & 0 & C_{28} \\ 0 & 0 & C_{33} & 0 & C_{35} & 0 & C_{37} & 0 \\ 0 & 0 & 0 & C_{44} & 0 & C_{46} & 0 & C_{48} \\ 0 & 0 & 0 & 0 & 1 & 0 & 0 & 0 \\ 0 & 0 & 0 & 0 & 0 & 1 & 0 & 0 \\ 0 & 0 & C_{73} & 0 & C_{75} & 0 & C_{77} & 0 \\ 0 & 0 & 0 & C_{84} & 0 & C_{86} & 0 & C_{88} \end{bmatrix} \begin{Bmatrix} x \\ y \\ \psi_x \\ \psi_y \\ V_x \\ V_y \\ M_x \\ M_y \end{Bmatrix}_n^R \tag{18}$$

where

$$\begin{aligned} C_{13} &= C_{24} = C_{75} = C_{86} = \ell \frac{\sin k}{k} \\ C_{15} &= C_{26} = \frac{\ell}{P}\left(1 - \frac{\sin k}{k}\right) \\ C_{17} &= C_{28} = C_{35} = C_{46} = \frac{1}{P}(1 - \cos k) \\ C_{33} &= C_{44} = \cos k \\ C_{37} &= C_{48} = \frac{k}{P\ell}\sin k \\ C_{73} &= C_{84} = -P\ell \frac{\sin k}{k} \\ C_{77} &= C_{88} = \cos k \end{aligned}$$

In more compact form,

$$\{X\}_{n+1}^L = [T_s]_n \{X\}_n^R \tag{19}$$

The overall transfer matrix can be found as

$$\prod_{i=n-1}^{1} [T_s]_i [T_m]_i = [T_s]_{n-1} [T_m]_{n-1} [T_s]_{n-2} [T_m]_{n-2} \cdots\cdots [T_s]_1 [T_m]_1 \tag{20}$$

3. Numerical Examples

A computer program was developed by employing the transfer matrix approach described in the previous section. Numerical analyses were conducted to investigate the effects of the axial force on both the natural frequency and the stability of general overhung rotor systems. The accuracy of the numerical solutions obtained from the developed computer program was tested by considering simple models for which exact solutions are available. For this purpose, the effect of applied forces on the critical speeds of

uniform shafts supported on either rigid short or rigid long bearings was investigated for comparison. When ten segments are used for the transfer matrix method, the maximum errors in the first two critical speeds are less than 0.02% for the shaft on short bearings and 0.04% for the shaft on long bearings.

3.1 Whirl Speeds of a Cantilevered Overhung Rotor under Axial Forces

The following data which represent one stage of a typical modern high-speed turbomachine were selected for the numerical analyses: shaft length ℓ = 0.254 m, shaft diameter d = 0.038 m, shaft density ρ = 7833 kg/m^3, disk mass m_d = 31.8 kg, disk polar moment of inertia I_p = 0.18 kg·m^2, disk transverse moment of inertia I_t = 0.09 kg·m^2, Young's modulus E = 2x10^{11} N/m^2, and shaft speed Ω = 7000 rpm. Using these data, eleven stations (ten elements of equal length for the shaft and one for the disk) were employed in the transfer matrix program to generate the results.

Fig. 3 shows the effect of axial force on the natural frequencies of a rotating shaft with and without a disk. The first natural frequency of a shaft without a disk decreases with increasing the compressive axial force and approaches zero at P=2.47EI/ℓ^2 that is the static buckling load for the non-rotating cantilevered beam. The eigenvalues of the first mode of the system become positive real numbers if the axial force is greater than the static buckling load. This implies that the system loses the stability without oscillation like a non-rotating Euler beam and shows divergence instability. For a cantilevered shaft with a disk, the natural frequency for each mode was split into two whirl frequencies due to the gyroscopic effect of a disk. All these whirl frequencies decrease as the axial force increases until the first backward whirl frequency (1B) becomes zero at P = 2.47EI/ℓ^2. Further increasing the compressive axial force, a new forward whirl frequency appears and increases while the existing first forward whirl frequency (1F) deceases continuously. This existing forward whirl frequency is now referred to as the second forward whirl frequency (2F) since a new lower forward whirl frequency appears for P > 2.47EI/ℓ^2. The new first forward whirl frequency coalesces with the second forward whirl frequency at P=2.58EI/ℓ^2. After coalescing, the eigenvalues of the first mode of the overhung rotor system become complex number and the negative logarithmic decrement appears as shown in Fig. 4. The figure presents the variation of the logarithmic decrement of the first mode of the overhung rotor for two different values of Q. As shown in the figure, the magnitude of the logarithmic decrement of the rotor system increases as the axial force increases after the first two forward whirl frequencies are coalesced at P=2.58EI/ℓ^2 and 2.82EI/ℓ^2 for Q = 0.044 and 0.088, respectively. This implies that the overhung rotor system loses the stability by oscillation with increasing amplitude and shows flutter instability after coalescing. Therefore, the critical axial force for flutter instability of an overhung rotor can be determined from coalescing of the first two forward frequencies. The gyroscopic effect of a rotor not only increases the critical force by stiffening the shaft but changes the instability type from divergence to flutter. Similar phenomena were obtained by utilizing the finite element method for a shaft without a

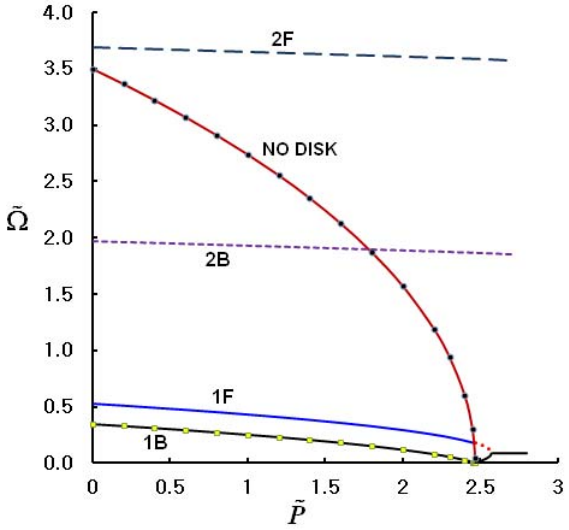

Fig. 3 Effect of axial force on the natural frequencies of the cantilevered overhung rotor (Q = 0.044)

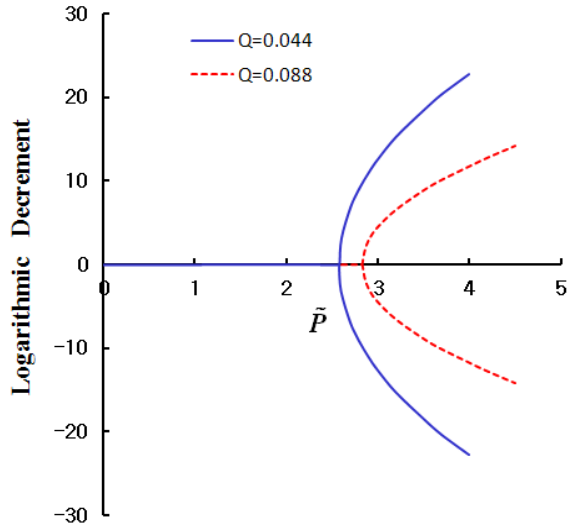

Fig. 4 Effect of axial force on the logarithmic decrement of the first mode of the cantilevered overhung rotor

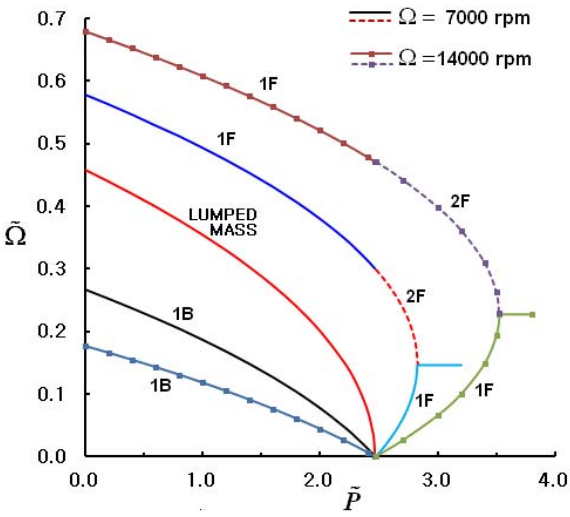

Fig. 5 Effect of the gyroscopic moment on the natural frequencies of an overhung rotor under axial forces (Q = 0.088)

disk in reference[6] and the lumped mass model for a rotor under periodic forces in reference.[8] The change in whirl frequencies for the second mode of the system is less than 5 percent when the compressive axial force is under the static bucking load.

The gyroscopic effect was further studied by increasing the moment of inertia of the disk and the rotating speed. As shown in Fig. 5, the stronger gyroscopic effect spaces the backward and forward frequencies further apart and moves the coalescing point between first two forward frequencies to a larger axial force of $P = 2.82EI/\ell^2$ when the moment of inertia of the disk is doubled, and $P = 3.52EI/\ell^2$ when both the moment of inertia of the disk and the rotating speed are doubled. However, the first backward frequency disappears at the same axial force which is the static buckling load of a shaft. A cantilevered shaft with a lumped mass was also considered to eliminate the gyroscopic effect of a disk. The first natural frequency of the rotor becomes zero at the static buckling load and the divergence instability occurs like the cantilevered shaft without a disk. The mass of the disk reduces the natural frequencies of the system but has no effect on the critical axial force for divergence instability at all. Therefore, the critical axial force for divergence instability is independent of the rotating speed and the mass of the disk. Such a critical axial force can be directly obtained by using the conventional buckling formulation.

3.2 Whirl Speed of an Overhung Rotor with an Intermediate Support under Axial Forces

An overhung rotor system with an intermediate support as shown in Fig. 6 is considered to simulate a typical single-stage overhung compressor supported by a rigid long bearing and a rigid short bearing or by two rigid short bearings. The effect of the support location was investigated by using the same data chosen for the cantilevered rotor. Fig. 7 shows the dimensionless natural frequencies of the rotor under axial forces for two different boundary conditions when the intermediate support is located at the middle of the shaft. Similar graphs and phenomena to the ones without an intermediate support were obtained. When the left end is supported by a rigid short bearing, the first backward frequency becomes zero at $P = 5.44EI/\ell^2$ and the first two forward frequencies coalesce at $P = 5.80EI/\ell^2$. These two axial forces increase to $6.27EI/\ell^2$ and $6.67EI/\ell^2$, respectively when the left end is supported by a rigid long bearing. The effect of the intermediate support on the critical force for instability can be determined by considering the axial force when the first backward whirl frequency disappears since the gyroscopic effect is constant for a given rotor operated at constant speed.

Fig. 8 presents the axial forces that make the first backward frequency zero for various locations of an intermediate support. The dimensionless term of ε denotes the ratio of ℓ_s, the length between the two supports, to the entire shaft length of ℓ. As can be seen in the figure, the difference between two different boundary conditions is less than 4% when the ratio of the length between two supports to the entire length of the shaft is less than 0.5. However, the difference increases sharply up to almost 100% as the support approaches to the free end of the shaft. Since these axial forces are independent of the rotating speed, the mass and the moment of inertia of the disk as observed in the previous case, they can be determined by considering the static buckling load for the corresponding system.

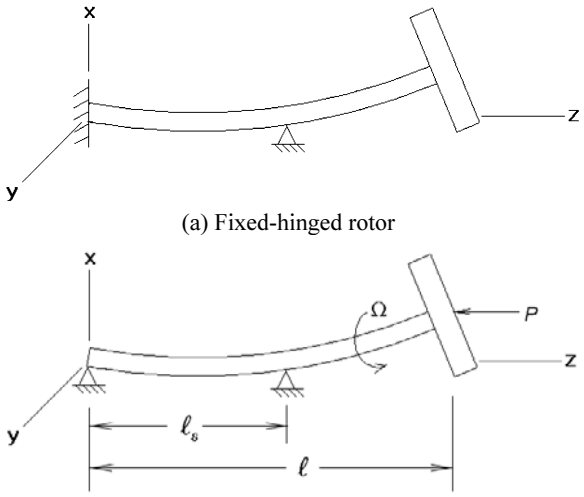

(a) Fixed-hinged rotor

(b) Hinged-hinged rotor

Fig. 6 An overhung rotor model with an intermediate support

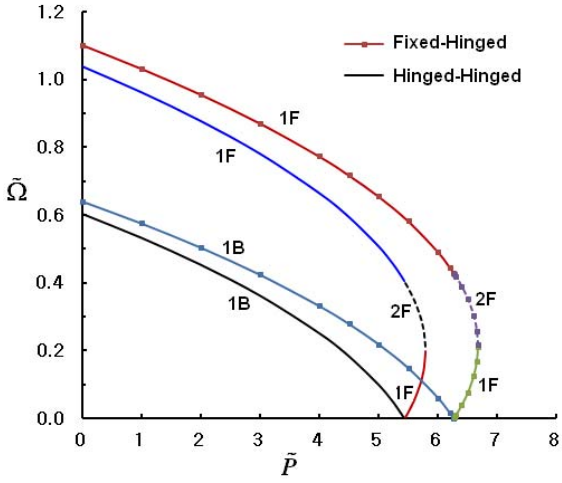

Fig. 7 Effect of axial force on the whirl frequencies of the overhung rotor for two different boundary conditions

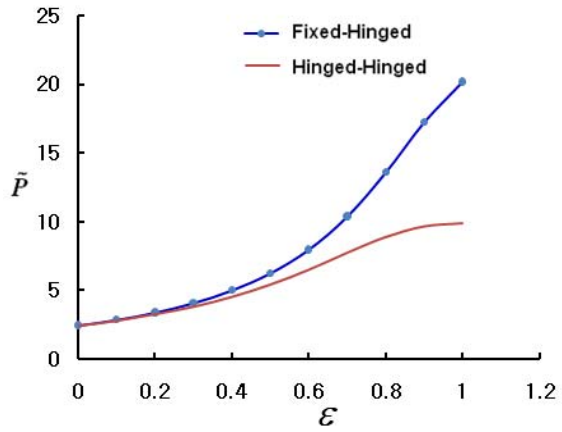

Fig. 8 The dimensionless axial force when the first backward whirl disappears for various locations of an intermediate support

4. Conclusions

The dynamic behavior of an overhung rotor under an axial force was studied by developing the transfer matrix for a flexible-shaft rotordynamic model. The following results were obtained by investigating the influence of the load force on the stability and the natural frequencies of overhung rotor systems.

1) The gyroscopic effect of the rotor strongly influences the dynamic behavior of the shaft-disk system under axial forces. The gyroscopic effect not only stiffens the shaft, and thus increases the critical axial force, but also changes the instability type from divergence to flutter.
2) The axial force that makes the first backward whirl frequency of the cantilevered overhung rotor with or without an intermediate support zero is independent of the rotating speed, the mass and the moment of inertia of the disk. Such an axial force can be determined by considering the static buckling load for a corresponding non-rotating Euler beam.

ACKNOWLEDGEMENT

This work was supported by Dongyang Mirae University.

REFERENCES

1. Saito, H. and Otomi, K., "Vibration and stability of elastically supported beams carrying an attached mass under axial and tangential loads," J. of Sound and Vibration, Vol. 62, No. 2, pp. 257-266, 1979.
2. Ari-Gur, J. and Elishakoff, I., "On the Effect of Shear Deformation on Buckling of Columns with Overhang," J. of Sound and Vibration, Vol. 139, No. 1, pp. 165-169, 1990.
3. Wang, C. M., Ng, K. H., and Kitipornchai, S., "Stability Criteria for Timoshenko Columns with Intermediate and End Concentrated Axial Loads," J. of Constructional Steel Research, Vol. 58, No. 9, pp. 1177-1193, 2002.
4. Arboleda-Monsalve, L. G., Zapata-Medina, D. G., and Aristizabal-Ochoa, J. D., "Stability and Natural Frequencies of a Weakened Timoshenko Beam-column with Generalized End Conditions under Constant Axial Load," J. of Sound and Vibration, Vol. 307, No. 1-2, pp. 89-112, 2007.
5. Cho, M. K. and Kim, C., "Dynamic Analyses of Fluctuating Bearing Forces on Worm Gears of Speed Reducers," Int. J. Precis. Eng. Manuf., Vol. 13, No. 2, pp. 193-199, 2012.
6. Ku, D.-M. and Chen, L.-W., "Stability and Whirl Speeds of Rotating Shaft under Axial Loads," International J. of Analytical and Experimental Modal Analysis, Vol. 9, No. 2, pp. 111-123, 1994.
7. Czołczyński, K. and Marynowski, K. P., "Instabilities of the elastically supported laval rotor subjected to a longitudinal force," J. of Sound and Vibration, Vol. 154, No. 2, pp. 281-288, 1992.
8. Sheu, H. C. and Chen, L. W., "Lumped mass model for parametric instability analysis of cantilever shaft-disk systems," J. of Sound and Vibration, Vol. 234, No. 2, pp. 331-348, 2000.
9. Yim, K. B., Noah, S. T., and Vance, J. M., "Effect of Tangential Torque on the Dynamics of Flexible Rotors," ASME J. of Applied Mechanics, Vol. 53, No. 3, pp. 711-718, 1986.